COBEM 2021 26th International Congress of Mechanical Engineering
ABCM Associação Brasileira de Engenharia e Ciências Mecânicas
November 22-26, 2021, Virtual Congress, Brazil

COB-2021-1869
DIMENSIONAL OPTIMIZATION OF AN UAV GRIPPING DEVICE

Rodrigo Cerqueira de Campos
Estevan Hideki Murai
Henrique Simas
Universidade Federal de Santa Catarina, Florianópolis SC 88040-900, Brazil
rodrigo.c.campos@posgrad.ufsc.br

Abstract. *Unmanned aerial vehicles (UAVs) are increasingly popular among different applications, mainly due to their mechanical simplicity and relatively low cost. Even though many obstacles still must be overcome, the employment of UAVs in logistics and transportation of packages has experienced substantial growth over the last few years. The development of new navigation and control technologies turned UAVs into a viable, cost-effective, and sustainable delivering option. Although the technology already offers the advantage of speed, flexibility, and ease in delivering goods, the interest in developing gripping systems that allow picking up cargo, either remotely or autonomously, is also high. Recently, different designs for autonomous landing platforms with safe positioning and fixation have been proposed. This paper aims to carry out the dimensional optimization of a passive UAV gripping device. The mechanism relies on the UAV's weight as an actuator to securely grab the cargo and springs that assist the opening motion. First, the kinematic modeling of the mechanism based on Natural Coordinates (NC) is performed. This model resulted in a non-linear system of equations, which was solved through the Newton-Raphson numerical method. The kinematic model was implemented in an algorithm developed in Python. The optimization process must take into account the full range of motion of the mechanism. Hence, a successive displacement analysis is performed to fully determine the motion of the device. Finally, dimensional optimization is accomplished by adopting the Genetic Algorithm (GA) process. The cost function is defined based on the desired path for the end-effector, while the penalties are set based on the allowable workspace. The GA algorithm was implemented in Python, and the results are evaluated through a CAD model.*

Keywords: *UAV, gripping device, natural coordinates, dimensional optimization, genetic algorithm.*

1. INTRODUCTION

Unmanned aerial vehicles (UAVs) have proven themselves as advanced tools for a variety of applications. Even though their use started in the military, they are also currently involved in the civil and commercial sectors. Due to their characteristics, UAVs represent a solution for many kinds of tasks, including transport (Kotarski *et al.*, 2020). The technological advance of the last few decades enabled the development of systems and components responsible for a significant leap in autonomous vehicles and robotics. Components with higher processing speed and integrated MEMS sensors provide better autonomy of the vehicle, while the enhancement of propulsion systems and batteries technologies enabled a wider range of applications (Kotarski *et al.*, 2020). These breakthroughs permitted the design of new controllers to perform aggressive maneuvers and to navigate in cluttered scenarios.

Different categories of UAVs are employed for different tasks and are the subject of many types of research. We have witnessed progressive advances in the field of UAVs, which include new technologies that enable multirotors to grasp, manipulate and transport objects. There are multiple applications in which UAV load transportation is useful, like package transportation in urban areas, application of pesticides in precision agriculture, and supplies delivery in conflict zones. Villa *et al.* (2019) argues that the use of multirotors for cargo transportation attends commercial, military, and civilian interests.

Although the employment of UAVs to load transportation is a promising solution, working with them is still quite challenging. The transport of goods has been accomplished by adopting two major carrying strategies. First, the works of Kotaru *et al.* (2018) suggested the suspension of the cargo to the UAV body through cables. This approach has also been adopted by other researchers and successfully implemented by commercial delivery companies. However, the cable-suspended load increases the number of under-actuated degrees of freedom, resulting in modified system dynamics. The second primary strategy consists of attaching the load to the multirotor body. This approach, on the other hand, increases the vehicle inertia, making it unfit for fast responses and agile maneuvers (Villa *et al.*, 2019).

Encouraged by recent developments in the field of UAVs cargo transportation, this paper aims to develop the dimensional optimization of a coupling device designed to attach a load to the UAV's body. First, a description of the studied mechanism is presented in Section 2., where the construction characteristics and working principles are highlighted. Afterwards, the steps taken to develop the optimization algorithm is described along Section 3. Finally, Section 4. presents a summary of the parameters adopted in the algorithm, and the results obtained.

2. MECHANISM DESCRIPTION

The coupling device studied in this paper is presented in Fig. 1. It is passively actuated, relying on the gravitational effect to accomplish the connection of the UAV to the external body. It is composed of four fingers, all of which are actuated simultaneously by a passive prismatic joint located at the center of the mechanism. As the UAV lands on top of the central base, the UAV's weight activates the prismatic joint, generating the closing motion.

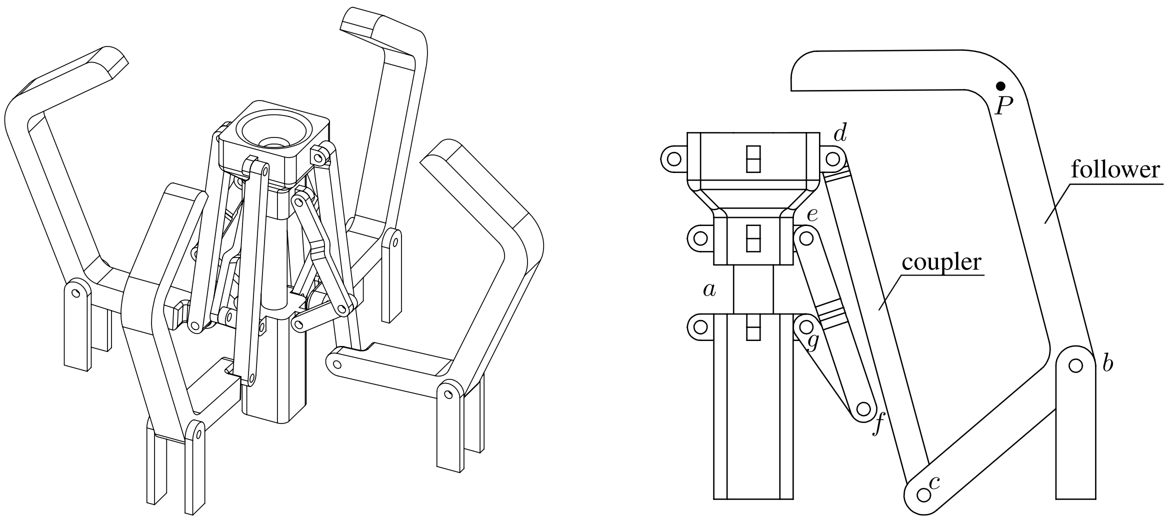

(a) Isometric view. (b) Front view of a single finger.

Figure 1: Coupling device topology.

Each finger can be identified in Fig. 1b by loop $bcdP$. It is constructed with a coupler link, connected to the centered prismatic joint, responsible for the force transmission to the follower, which is connected to the coupler link and to the fixed frame. All connections are made with revolute kinematic pairs. The end-effector, denoted in Fig. 1b as P, is considered as a point on the outer limit of the finger contact surface. It performs a circular motion, where the radius is the length of the follower and the center is the revolute joint that connects the follower to the fixed frame.

Figure 1a shows a conic opening on the top of the centered base. Similarly, a conic support is attached to the UAV, through which the connection is established. Figure 2a presents the UAV descending towards the gripping device, while Fig 2b shows the system in a closed state. The conic geometry assists the UAV in getting a better alignment and ensures a steady connection and a firm grip.

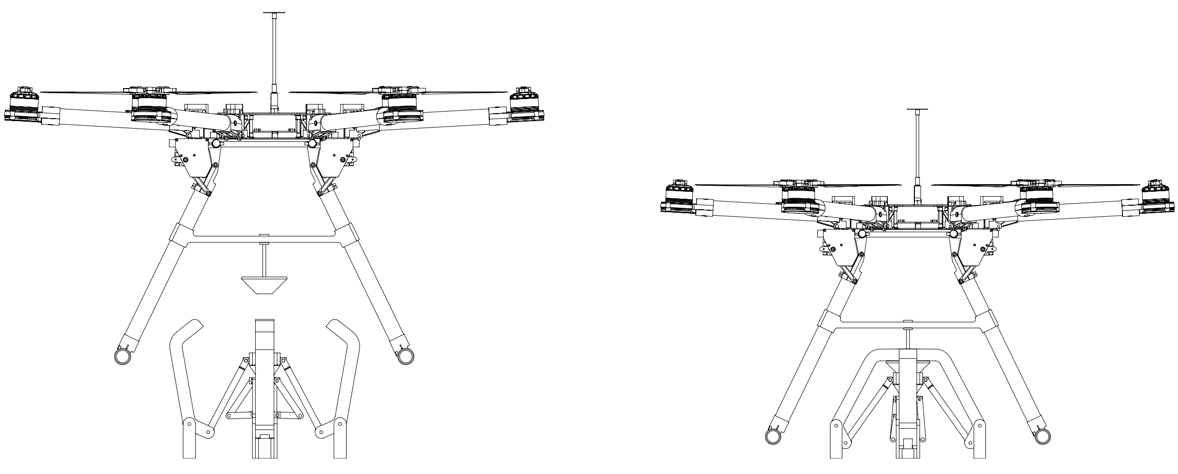

(a) Open state. (b) Closed state.

Figure 2: Coupling process.

Considering the range of applications in which this kind of device may be employed, such as aerial transport, it is of most importance that after the correct coupling, the system remains locked together, safe from accidental disconnections.

In order to provide this kind of safety, the gripper has a locking device that can be identified on Fig. 1 by loop $aefg$. As the mechanism performs the closing motion, a torsion spring placed on joint g stores enough energy to open the gripper when desired. As the mechanism reaches the fully closed position, a solenoid fixes joint f, preventing any undesired motion. In order to release the gripper from its locked position, an electrical signal is sent to the solenoid, releasing this external constraint. Afterwards, the twisted torsion spring performs as an actuator to open the mechanism to its original state.

This mechanism resembles a multi-finger gripper. It was designed to be positioned in the internal region of the UAV's landing gear, as illustrated by Fig. 2. It should be noted that the process of positioning the UAV at the desired point on the coupling device begins during its flight, where it usually adjusts its position to land at a given point. The deviation between the desired landing position and the actually achieved position depends on the sensors installed in the vehicle, the chosen landing technique, the controlling system's performance, and other unpredictable external factors, such as meteorological conditions. This paper focuses exclusively on the mechanics of the coupling mechanism.

3. DIMENSIONAL OPTIMIZATION

Generally, the dimensional synthesis of mechanisms involves nonlinear equations and workspace discontinuities, resulting in a highly complex task. Therefore, the use of an optimization process is often adopted. Many recent studies adopted this technique, such as Wang *et al.* (2019), who used Genetic Algorithm to enhance the kinematic performance of a 3-DOF redundantly actuated parallel mechanism designed for lower-limb rehabilitation, and Chablat *et al.* (2018), who adopted a multi-objective optimization using Genetic Algorithm to minimize the size of a pipe inspection robot, while maximizing the force transmission from the actuators.

This paper employs the Genetic Algorithm to perform the dimensional optimization of the coupling device presented in Section 2., in order to ensure that the mechanism securely fits in the internal region of the UAV's landing gear. It is considered that the coupling device will be used with a DJI Spreading Wings S900 UAV, and the dimensional optimization of the gripper adopts the geometrical specifications provided by its manufacturer. However, the same optimization process applies to any other UAV model. From Fig. 1a, it can be seen that the mechanism is perfectly symmetric. Hence, the optimization process may be applied to a single finger.

3.1 Kinematic analysis

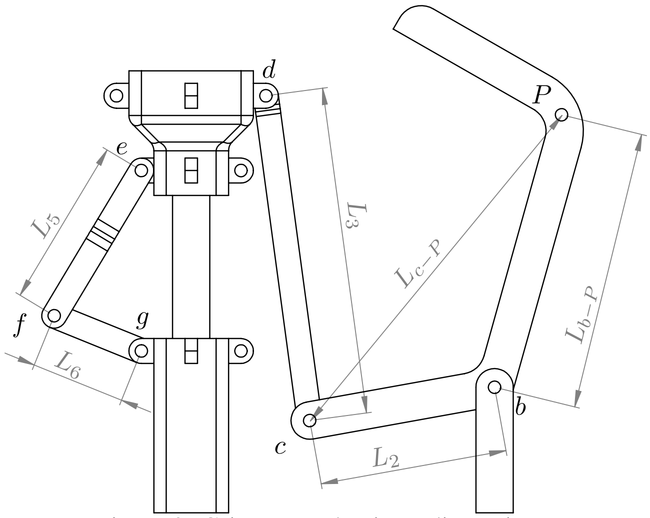

Figure 3: Gripper mechanisms dimensions.

The kinematic analysis of multibody systems is generally achieved through a geometrical approach, where a vector-loop equation is defined for each loop of the mechanism. This method has been successfully applied by several authors, such as Lian *et al.* (2015) who analyzed the stiffness of a 5-DOF Parallel Manipulator. It presents, however, two significant drawbacks. First, along with the development of the analysis, the coordinates of every passive joint are eliminated, resulting in a direct relationship between input and end-effector. These coordinates, however, are necessary to perform the dimensional optimization. Second, the high degree of nonlinearity of the governing equations results in a complex computer implementation, as explained by Xu *et al.* (2021).

In order to reduce the mathematical complexity of the resulting system of equations and get the coordinates of all passive joints, the inverse kinematics was developed through Natural Coordinates (NC). As exposed by Nuñez *et al.* (2014), a few of the major advantages of adopting this method are the easier and more systematic application, and results in less complex equations.

Through Fig. 3, applying the NC modelling method results in the following equations:

$$\begin{cases} (x_b - x_c)^2 + (y_b - y_c)^2 = L_2^2 \\ (x_c - x_d)^2 + (y_c - y_d)^2 = L_3^2 \\ (x_b - x_P)^2 + (y_b - y_P)^2 = L_{b-P}^2 \\ (x_c - x_P)^2 + (y_c - y_P)^2 = L_{c-P}^2 \\ (x_e - x_f)^2 + (y_e - y_f)^2 = L_5^2 \\ (x_f - x_g)^2 + (y_f - y_g)^2 = L_6^2 \end{cases}, \tag{1}$$

where the subscript P represents the end-effector.

It should be noted that, for the locking device, the dimensions of links L_5 and L_6 do not require optimization. Since the final position of joint f is known, as stated in Section 2., the calculation of L_5 and L_6 is straightforward. Therefore, the system of equations used in the optimization process is reduced to

$$\begin{cases} \phi_1 = (x_b - x_c)^2 + (y_b - y_c)^2 - L_2^2 \\ \phi_2 = (x_c - x_d)^2 + (y_c - y_d)^2 - L_3^2 \\ \phi_3 = (x_b - x_P)^2 + (y_b - y_P)^2 - L_{b-P}^2 \\ \phi_4 = (x_c - x_P)^2 + (y_c - y_P)^2 = L_{c-P}^2 \end{cases}. \tag{2}$$

In order to systemize the computation procedure, the system of equations given by Eq. (1) is rewritten in a matrix form,

$$\mathbf{\Phi}(\mathbf{q}, \mathbf{z}, \phi) = \begin{bmatrix} \phi_1(\mathbf{q}, \mathbf{z}, \phi) \\ \phi_2(\mathbf{q}, \mathbf{z}, \phi) \\ \vdots \\ \phi_m(\mathbf{q}, \mathbf{z}, \phi) \end{bmatrix} = \mathbf{0}, \tag{3}$$

where the vector $\mathbf{q}$ contains all the unknown variables, vector $\mathbf{z}$ contains the dimensions of the links L_2, L_3 and L_{b-P}, ϕ is the input which represents the mechanism's degree of freedom and m is the number of equations.

Since we have a nonlinear system of equations, it is not possible to solve them analytically, so an iterative method is required. The Newton-Raphson numerical method was adopted, and its computing method is described as,

$$\mathbf{q_{i+1}} = \mathbf{q_i} + \nabla\mathbf{\Phi}(\mathbf{q_i}, \mathbf{z}, \phi)^{\mathbf{-1}}\mathbf{\Phi}(\mathbf{q_i}, \mathbf{z}, \phi), \tag{4}$$

where $\nabla\mathbf{\Phi}(\mathbf{q_i}, \phi)$ is the jacobian matrix of the equation vector Φ, given by

$$\nabla\mathbf{\Phi}(\mathbf{q_i}, \mathbf{z}, \phi) = \begin{bmatrix} \frac{\partial\phi_1}{\partial q_1} & \frac{\partial\phi_1}{\partial q_2} & \cdots & \frac{\partial\phi_1}{\partial q_n} \\ \frac{\partial\phi_2}{\partial q_1} & \frac{\partial\phi_2}{\partial q_2} & \cdots & \frac{\partial\phi_2}{\partial q_n} \\ \vdots & \vdots & \ddots & \vdots \\ \frac{\partial\phi_m}{\partial q_1} & \frac{\partial\phi_m}{\partial q_2} & \cdots & \frac{\partial\phi_m}{\partial q_n} \end{bmatrix}. \tag{5}$$

It can be seen from Eq. (4) that, in order to start the calculation process, a set of existing points for the unknown variables is needed. Hence, an initial guess for $\mathbf{q_0}$ must be provided.

3.2 Successive displacements

In order to guarantee that the final mechanism works properly, the dimensional optimization must consider the entire range of motion performed by the coupling device. Once the initial position has been established, the successive displacements may be computed by adopting the last position as an initial guess, provided that the displacements are small enough.

Considering $\mathbf{q_0}$ is a known initial position. The next following positions may be determined as,

$$\mathbf{q_1} = \mathbf{q_0} + \nabla\mathbf{\Phi}(\mathbf{q_0}, \phi)^{\mathbf{-1}}\mathbf{\Phi}(\mathbf{q_0}, \phi), \tag{6}$$

$$\mathbf{q_2} = \mathbf{q_1} + \nabla\mathbf{\Phi}(\mathbf{q_1}, \phi)^{-\mathbf{1}}\mathbf{\Phi}(\mathbf{q_1}, \phi). \tag{7}$$

Hence, the $n - ith$ position can be computed by

$$\mathbf{q_n} = \mathbf{q_{n-1}} + \nabla\mathbf{\Phi}(\mathbf{q_{n-1}}, \phi)^{-\mathbf{1}}\mathbf{\Phi}(\mathbf{q_{n-1}}, \phi). \tag{8}$$

3.3 Dimensional requirements

As described in Section 2., when the gripper is closed, it lies inside the UAV's landing gear, which is also supported by the lower surface. Hence, it is important that the length of the links are in a suitable size. Also, collisions of the coupling device's finger with the landing gear during the closing motion should be avoided. Figure 4 presents the UAV's landing gear dimensions. This way, it is possible to determine the maximum x_P coordinate to avoid collision based on the y_P coordinate through

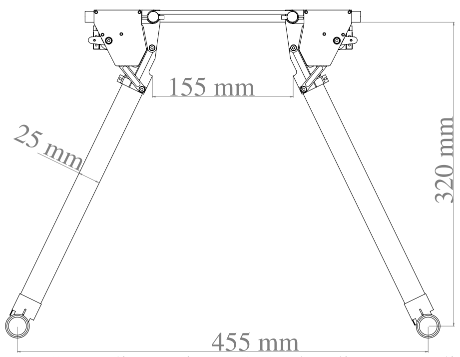

Figure 4: DJI Spreading Wings S900 landing gear dimensions.

$$x_P < \frac{485.3258 - y_P}{2.1333}. \tag{9}$$

The transmission quality μ is an indicator of the mechanism's effectiveness. It may be determined by measuring the angle between the coupler and follower links. As exposed by Martins and Murai (2019), it is recommended that the angle μ stays in the range of 40° to 140°. Hence, the transmission quality can be calculated through the cosine law,

$$\mu = cos^{-1}\frac{L_{bd}^2 - L_3^2 - L_2^2}{2L_2L_3}, \tag{10}$$

where L_{bd} is the distance between joints b and d.

3.4 Genetic algorithm

Genetic Algorithm (GA) is a search and optimization method based on genetic principles and natural selection (Nuñez *et al.*, 2014). It allows a population composed of many individuals to evolve based on pre-defined rules. The optimization process through GA can be summarized in defining the cost function, in which the variables limits and GA parameters are defined, initial population generation, computing the cost function for each individual, selection, mating, mutation and finally, convergence checking. The optimization process adopted closely follows the works of Nuñez *et al.* (2014) and Weihmann (2011), which provides a more detailed description of the Genetic Algorithm.

3.4.1 Cost function

The GA requires the definition of a cost function $f(\mathbf{q})$, where the minimum value of $f(\mathbf{q})$ indicates that the mechanism behaves as intended. An optimization problem may be mathematically described as

$$\begin{aligned} &\text{minimize } f(\mathbf{q}) \\ &\text{subject to } \mathbf{g}(\mathbf{q}) \leq 0, \\ &\qquad\qquad \mathbf{h}(\mathbf{q}) = 0 \end{aligned} \tag{11}$$

where $\mathbf{g}(\mathbf{q})$ is the inequalities restrictions vector and $\mathbf{h}(\mathbf{q})$ is equalities restrictions vector.

Generally, the cost function is composed of the error between the achieved path of the end-effector and the desired path. However, in this case, the path is known to be circular, where the center of the circle is the coordinates of joint b and the radius is the distance of joint b to the end-effector, which are not known. Therefore, it is not possible to fully define the desired path.

Although the desired path is not known beforehand, it is possible to define that, in the closed position, the end-effector is positioned right above joint d. This way, it is possible to define that the quadratic error between the desired position and the achieved position when the gripper is closed should be minimal. Then, the cost function $f(\mathbf{q})$ can be written as

$$f(\mathbf{q}) = (x_P - x_{P_{desired}})^2 + (y_P - y_{P_{desired}})^2, \tag{12}$$

There is nothing to be optimized on the path traveled by the end-effector as the gripper opens. There are, however, some limits imposed by the UAV landing gear, as discussed in Section 3.3. These limits are added to the cost function as penalty functions $P(\mathbf{q})$. Then, if the results obtained in a given iteration break these limits, the cost function suffers a penalty, so the GA tries to avoid these problems in the next iterations. This way, Eq. (12) can be rewritten as,

$$\text{minimize } f(\mathbf{q}) + \sum_{1}^{k} P(\mathbf{q}). \tag{13}$$

where k is the number of penalty functions. Considering the dimensional constraints discussed in Section 3.3, the gripping device has two boundaries. The first one is regarding the landing gear dimensions, which has to respect the limits imposed by Eq. (9) to avoid a collision between the gripper's finger and the landing gear. The second one is regarding the transmission quality μ, given by Eq. (10). Even though it is not mandatory, it is desirable that μ is as close as possible to the recommended range.

3.4.2 Design parameters

Although the idea of a dimensional optimization process is to find a solution that best fits the desired outcome, some design parameters have to be determined prior to the optimization to define the mechanism's topology better and reduce computational costs. In this case, the height of the closed gripper is set to 130 mm, without considering the thickness of the follower. Although this definition is somewhat arbitrary, keeping the mechanism in the lower portion of the landing gear provides a wider range for the fingers motion and avoids the possibility of collision to the UAV's battery. The coordinates for joint d are also set to $x_d = 30$ mm and $y_d = 110$ mm, considering that the coupler attached to the UAV is 20 mm thick. Hence, the desired position for the end-effector in a closed state is $x_{P_{desired}} = 40$ mm and $x_{P_{desired}} = 130$ mm.

Considering the definitions above, the system of equations given by Eq. (2) is left with 5 unknowns: L_2, L_3, L_{c-P}, x_b, y_b. The value of L_{b-P} can be calculated by

$$L_{b-P} = \sqrt{(x_{P_{desired}} - xb)^2 + (y_{P_{desired}} - yb^2)}. \tag{14}$$

The coordinates for joint c and the achieved end-effector position P vary throughout the gripper's motion. However, as stated before, it is still necessary to provide the algorithm with an initial guess. The optimization algorithm starts with the gripper's closed position. Hence, the initial guess for the end-effector may be a value close to the desired position specified above. The initial guess for joint c, on the other hand, is not as straightforward. From Fig. 1b, it can be seen that joint c is positioned close to the ground, and between the prismatic center and joint b, which is currently unknown. Therefore, the chosen values were $y_c = 0$ and $x_c = 50$ mm, equivalent to $\frac{1}{4}$th of the available space in the x-axis. Hence, the vector $\mathbf{q_0}$ is given by

$$\mathbf{q_0} = \begin{bmatrix} 50 & 0 & 38 & 125 \end{bmatrix}. \tag{15}$$

For each variable, it is necessary to provide the algorithm with a range of values to search for the best solution. Figure 4 presents the dimensions of the UAV landing gear and, consequently, the maximum allowable values. Since none of the variables can physically accept negative numbers, nor zero, the lower bound is set to 10 mm, and the upper limit is set to 300 mm for the dimensions of the links, 210 mm to the x coordinate, and 100 mm to the y coordinate.

4. Results

The dimensional optimization described in this paper has been implemented in Python. All the design parameters related to the mechanism that were adopted prior to the optimization process mentioned in section 3.4.2 are summarized in Tab. 1. As mentioned in Section 3.4.2, the optimization problem has 5 unknowns. The population size was determined to be 50, a crossover rate of 70% and a mutation rate of 20%. The maximum number of iterations was established as 10000.

Table 1: Design parameters adopted.

x_d [mm]	y_d [mm]	x_P [mm]	y_P [mm]	Prismatic Joint Displacement [mm]
30	110	40	130	40

The optimization process took approximately two and a half hours to achieve convergence. As presented by Tab. 2, the results of the optimization process are satisfactory and realistic when compared to the dimensions of the landing gear.

Table 2: Results obtained from the GA.

L_2 [mm]	L_3 [mm]	L_{c-P} [mm]	x_b [mm]	y_b [mm]
38.8179	110.0973	123.3137	120.2957	44.3345

Figure 5 presents a plot of the trajectory performed by the end-effector, as well as a CAD model built with the results of the optimization process in a fully closed state (Fig. 5a), in a mid-opening state (Fig. 5b) and fully disconnected (Fig. 5c). It can be seen that the desired position for a closed state was achieved. Furthermore, in a fully open state, the x coordinate of the end-effector is reasonably distant from the lower part of the landing gear, which reduces the risk of collision during the landing process.

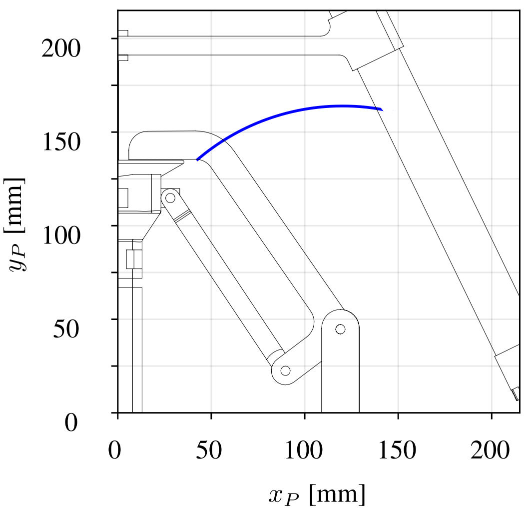

(a) Fully closed.

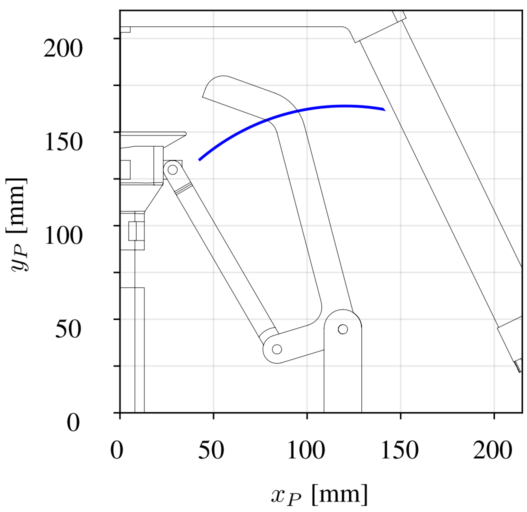

(b) Partially open.

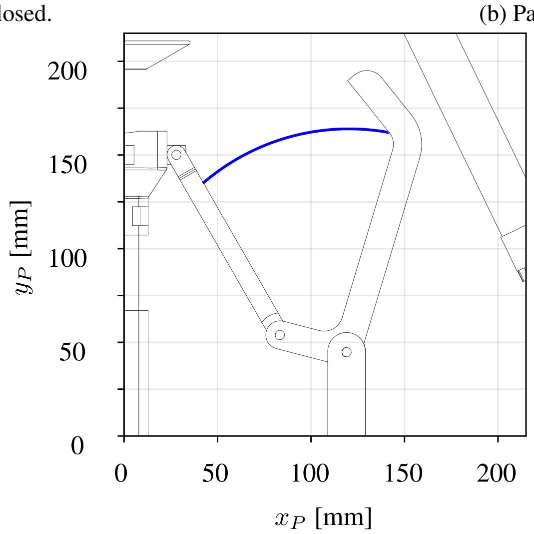

(c) Fully open.

Figure 5: CAD model with the optimized dimensions.

5. Conclusions

This paper presented a method for solving the topology optimization of a coupling device for unmanned aerial vehicles. The proposed procedure was based on the dimensional limits imposed by the selected UAV landing gear, which dimensions are provided by its manufacturer's website.

The position kinematic modeling and successive displacements were achieved by employing the Natural Coordinates method as a primary mathematical tool. This allowed to determine the position of every joint for several different positions, which were used by the Genetic Algorithm to evaluate each potential solution.

The method presented in this paper has been successfully implemented in Python. The results obtained were satisfactory considering the geometrical constraints, and the final mechanism presented itself as a potentially viable solution to the problem addressed. The present study may serve as a basis for the topological optimization of similar devices for different necessities or for applications with different UAVs. For future works, the structural optimization and stiffness analysis of this topology could be performed to better evaluate the possibilities of application in real-world scenarios.

6. REFERENCES

Chablat, D., Venkateswaran, S. and Boyer, F., 2018. "Mechanical design optimization of a piping inspection robot". *Procedia Cirp*, Vol. 70, pp. 307–312.

Kotarski, D., Piljek, P. and Kasać, J., 2020. "Design considerations for autonomous cargo transportation multirotor uavs". In *Self-driving Vehicles and Enabling Technologies*, IntechOpen.

Kotaru, P., Wu, G. and Sreenath, K., 2018. "Differential-flatness and control of quadrotor (s) with a payload suspended through flexible cable (s)". In *2018 Indian Control Conference (ICC)*. IEEE, pp. 352–357.

Lian, B., Sun, T., Song, Y., Jin, Y. and Price, M., 2015. "Stiffness analysis and experiment of a novel 5-dof parallel kinematic machine considering gravitational effects". *International Journal of Machine Tools and Manufacture*, Vol. 95, pp. 82–96.

Martins, D. and Murai, E.H., 2019. *Mechanisms synthesis ans analysis with applications in robotics (in Portuguese)*. Editora UFSC, Florianópolis.

Nuñez, N.N.R. *et al.*, 2014. "Síntese estrutural e otimização dimensional de mecanismos de direção".

Villa, D.K., Brandão, A.S. and Sarcinelli-Filho, M., 2019. "A survey on load transportation using multirotor uavs". *Journal of Intelligent & Robotic Systems*, pp. 1–30.

Wang, H., Li, W., Liu, H., Zhang, J. and Liu, S., 2019. "Conceptual design and dimensional synthesis of a novel parallel mechanism for lower-limb rehabilitation". *Robotica*, Vol. 37, No. 3, pp. 469–480.

Weihmann, L., 2011. *Modelagem e otimização de forças e torques aplicados por robôs com redundância cinemática e de atuação em contato com o meio. Florianópolis, 2011. 332 p.* Ph.D. thesis, Tese (Doutorado)-Universidade Federal de Santa Catarina, Centro Tecnológico . . . .

Xu, X., Luo, J., Feng, X., Peng, H. and Wu, Z., 2021. "A generalized inertia representation for rigid multibody systems in terms of natural coordinates". *Mechanism and Machine Theory*, Vol. 157, p. 104174.

7. RESPONSIBILITY NOTICE